EUROPEAN ORGANIZATION FOR NUCLEAR RESEARCH

CERN/EF 88-3
5 April 1988

ON ELECTRICAL BREAKDOWN IN SUPERCONDUCTING ACCELERATING CAVITIES

W. Weingarten

CERN, European Organization for Nuclear Research, 1211 Geneva 23, Switzerland

Abstract - Recent results on electron loading in superconducting cavities are presented and compared with observations in DC field emission.

INTRODUCTION

Accelerating cavities from superconducting Nb metal theoretically allow high accelerating fields at low losses. The superheating critical field being considered as the ultimate field limit [1], which for high purity Nb is 2000 G [2], accelerating fields of typically 50 MV/m should be at reach. However, experimentally obtained fields are still lower [2].

Since the early eighties diagnostical tools have been developed in order to investigate the physical reason underlying this discrepancy [3,4]. Three mechanisms have since emerged as field limitations: thermal breakdown, MultiPactor (MP) (or "resonant") electron loading and Field Emission (FE) (or "non resonant") electron loading.

Thermal breakdown has become less important, since thermally stable surfaces are available now (high thermal conductivity Nb sheet [5] and a thin Nb film on a Cu sheet [6]). Today, the electron loading is therefore the major obstacle towards higher accelerating fields.

MP electron loading (or "resonant" electron loading) has, in principle, been understood. It has largely been overcome by choosing the correct geometry of the accelerating structure ("rounded" cavity shape) [7,8].

However, in particular at frequencies used for storage ring application (below 1 GHz) and for surfaces with an enhanced secondary electron emission coefficient due to spurious contaminations, MP electron loading may still induce a limitation or breakdown of the accelerating field ("quench"). One has sometimes to abide by long processing times to pass through this threshold.

Compared to MP electron loading the understanding of FE electron loading (or "non resonant" electron loading) is at its infancy. Nevertheless, some cures have been found experimentally. DC FE studies have substantially contributed to the body of knowledge of electron loading. In any case it is a major task to process a cavity surface of some m^2 area such that it is completely free from even one single field emitter up to some target field level.

What does the term "electrical breakdown" mean? Either the electron loading is so strong that part of the cavity surface is driven normal by the heat produced by electron impact. The stored energy of the cavity is then dumped into that normal conducting surface, such that the accelerating field breaks down abruptly ("quench"). Or, on the other hand, the cavity losses increase with the accelerating field faster than the RF power needed to replace them. The accelerating field saturates, without a quench being observed.

Sparking, as observed in DC FE, was not observed in RF cavities. The drastic increase of RF losses by electron loading prevents to raise the RF field to produce a spark.

EXPERIMENTAL RESULTS FROM CERN ILLUSTRATING ELECTRON LOADING

To illustrate the field limitations due to electron loading (both MP and FE electron loading) I list in table 1 the sequence of the maximum accelerating field E_a^{max} of a prototype cavity for the CERN $e^{\pm}$ collider LEP (called "LEP2", fig. 1), which is actually being tested in the SPS accelerator [7].

The RF losses of a cavity are characterized by the Q-value. The RF losses per meter P/L for an accelerating cavity at a frequency f [GHz], Q [10^9] and an accelerating field E_a [MV/m] are $P/L \sim E_a^2/(Q.f)$.

As an illustration of the best results obtained at CERN, I list in table 2 the maximum accelerating fields for the different types of cavities under study. Fig. 2 shows the corresponding Q values vs. the accelerating field.

Four conclusions can be drawn from the results obtained in these RF cavities:

(a) MP electron loading, though sometimes limiting the accelerating field (table 1, # 4-7), can be overcome by a sufficiently long RF processing (operating the cavity at high field just below breakdown without He gas partial pressure).

XIIIth International Symposium on Discharges and Electrical Insulation in Vacuum
27-30 June 1988, Paris, France

(b) Extended time (50 to 70 h) had to be spent to increase the accelerating fields for the LEP prototype cavities (table 2, # 6 and 7) up and beyond the design field of 5 MV/m by He-processing (operating the cavity at high field just below breakdown under a He gas partial pressure of $\sim 10^{-5}$ mbar).

(c) The maximum accelerating fields (in particular before He-processing) are correlated with the total surface area of the cavity (fig. 3).

(d) There is no fundamental difference regarding FE electron loading between metal sheet and sputter coated Nb cavities (table 2, # 3 and 4, 6 and 7).

TABLE 1 - "LEP2" cavity cold tests

#	Surface treatment[a]	E_a^{max} [MV/m]	He-processing [h]	Field limit[b]	Remarks[c]
1	CP, W	5.7	20	e^- (FE)	L[d]
2	CP, W	4.0	40	e^- (FE)[e]	L
3	CP, C_2H_5OH, W	7.3	50	e^- (FE)	L
4	C_2H_5OH, W	4.5	10	e^- (MP)	SPS
5	-	4.2	-	e^- (MP)	SPS
6	-	4.3	4	e^- (MP)	SPS
7	-	4.4	-	e^- (MP)	SPS[f]
8	-	7.2	-	P	L
9	-	5.0	-	(g)	L
10	-	6.5	-	P	SPS

(a) CP = Chemical Polish, C_2H_5OH = alcohol rinsing, W = water rinsing.

(b) e^- (FE) = Field Emission electron loading.
e^- (MP) = MultiPactor electron loading.
P = Maximum RF power rating of some RF component (window, connector, etc).

(c) L = Laboratory test.
SPS = Cavity connected to SPS accelerator vacuum system.

(d) Leak at RF probe due to e^- impact.

(e) e^- (FE) by ceramic particles in cavity due to accident.

(f) Acceleration test.

(g) CW test at design field of 5 MV/m.

TABLE 2 - Maximum accelerating fields for accelerating cavities under study at CERN

#		f [MHz]	Material[a]	No. of cells	$E_a^{max(b)}$ [MV/m]	He-processing [h]	Field limit[c]	Surface area [m^2]
1	(H1)	500	Nb	1	9.8 → 13.8	2	P	.6
2	(8.2)	500	Nb/Cu	1	11.2 → 15.1	5	P	.6
3	(K2)	350	Nb	1	8.8 → 10.9	.5	P	1.2
4	(31)	350	Nb/Cu	1	5.3 → 7.2	5	e^-(FE)	1.2
5	(PETRA)	500	Nb	5	5.0	-	P	3.0
6	(LEP0)	350	Nb	4	2.0 → 7.5	70	e^-(FE)	4.8
7	(45)	350	Nb/Cu	4	2.0 → 7.0	33	e^-(FE)	4.8

(a) Nb = produced from high-thermal conductivity Nb sheet.
Nb/Cu = 1 µm Nb sputter coated on Cu sheet.

(b) The arrow indicates the improvement in the accelerating field by He-processing; the peak electric surface field $E_p = 2E_a$.

(c) Cf. table 1.

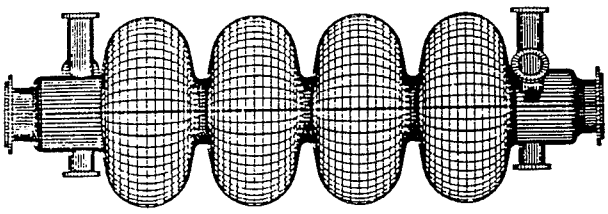

Fig. 1 - Superconducting LEP prototype accelerating cavity (LEP2) used in the CERN SPS accelerator. The whole unit has a length of 2.4 m.

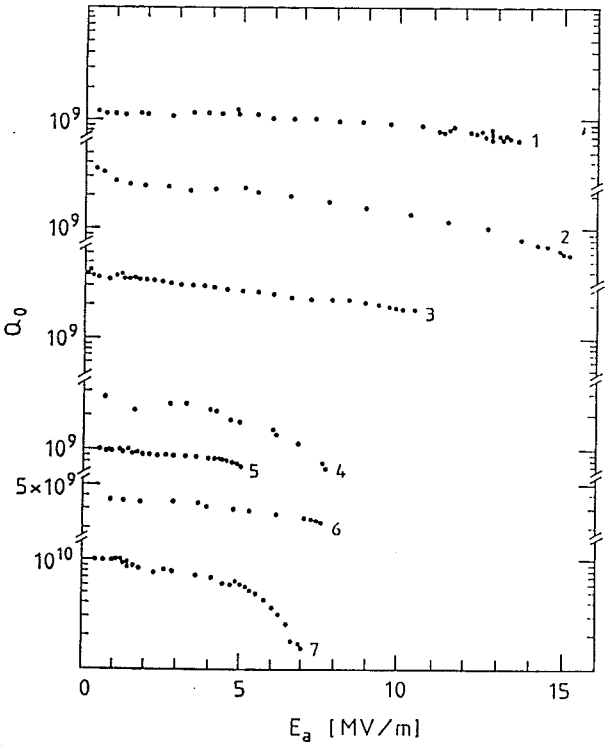

Fig. 2 - Dependence of the Q-value on the accelerating field E_α (for the accelerating cavities from table 2).

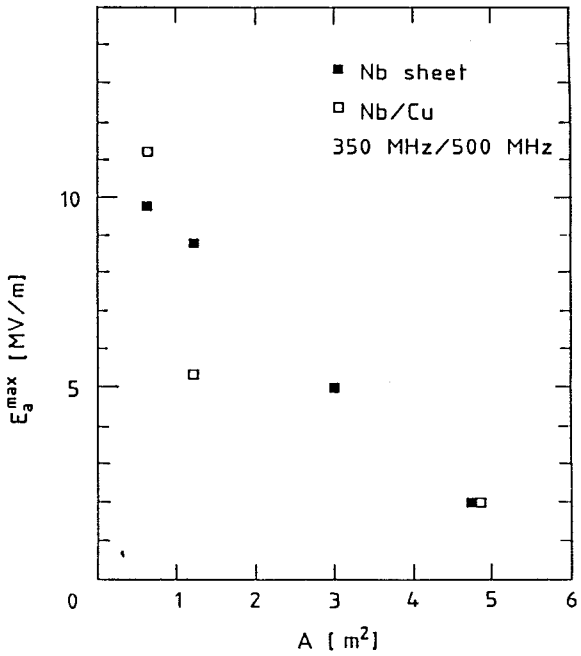

Fig. 3 - Correlation of the maximum accelerating field before He-processing with the cavity surface area (for the accelerating cavities from table 2).

MULTIPACTOR ELECTRON LOADING

For many years, one side electron multipacting [8] was a nuisance for superconducting cavities, up to the advent of cavities with the "rounded" shape [9,10]. They were virtually free from electron multipacting, provided that the secondary electron emission coefficient δ equals that of clean Nb surfaces. However, on real surfaces δ may be enhanced [11]. In fact, in 500 MHz single-cell cavities a two-side electron multipacting was found and analyzed [12]. It takes place near the zero crossing of the surface electric field at the equator of the cavity at 9.5 ± 2.0 MV/m (figs 4 and 5), if the maximum secondary electron emission coefficient exceeds 1.6 [13].

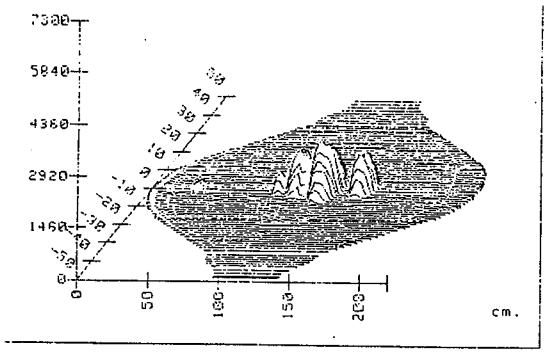

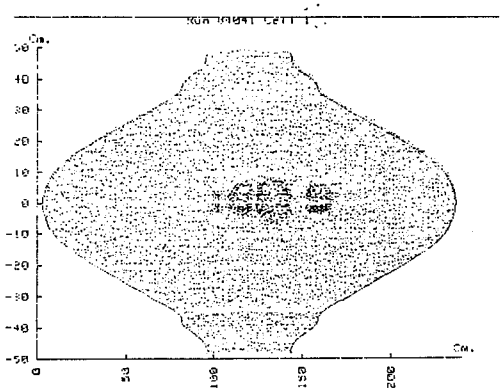

Fig. 4 - Temperature map of a 500 MHz monocell cavity in the moment of quenching due to MP electron loading near the equator.

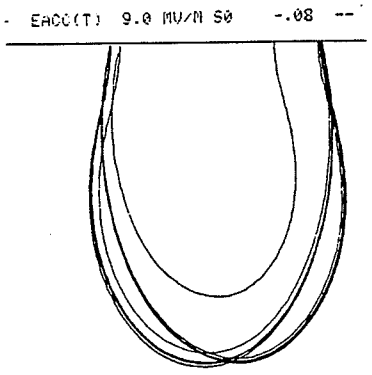

Fig. 5 - Computer simulation of electron trajectories for two-side electron multipacting at the equator. The distance of points of impact is 1 mm.

It can usually be suppressed by RF processing, which diminishes the secondary electron emission coefficient by electron bombardment [14]. As the electron multipacting threshold fields scale with frequency, at 350 MHz this type of multipacting is observed at 6.7 ± 1.4 MV/m. The enhanced losses it produces are clearly seen in a faster decay of the cavity voltage of a mono-cell 350 MHz cavity (fig. 6).

FIELD EMISSION ELECTRON LOADING

The FE electron loading current follows closely the Fowler-Nordheim theory of metallic field emission [15] provided that the local electric field was enhanced by the "field enhancement factor" β. About a decade ago it was thought to originate at metallic whiskers, spikes etc., at which the local electric surface field was enhanced by geometry. However, evidence for such spikes has never been conclusively found.

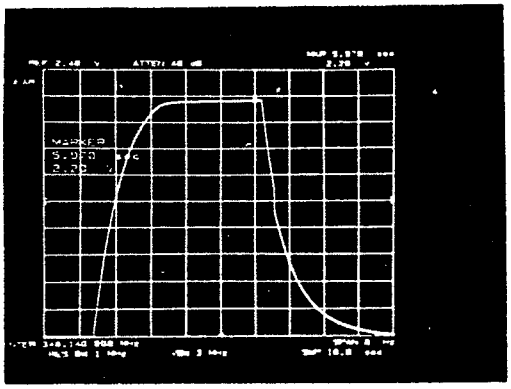

Fig. 6 - Fast decay of the accelerating field of a 350 MHz cavity near the multipacting threshold at 5 MV/m (full scale = 10 MV/m).

From DC FE studies it became clear, that the broad area FE was not caused by FE from a metallic object [16]. From RF cavity measurements, backed up by more powerful diagnostical tools, it became also clear, that FE sites were pointlike and only a few dispersed over a large area [17]. This could hardly be explained by metallic spikes or protrusions originating for example at the grain boundaries, being by far too numerous and densely distributed.

Diagnosing FE electron loading - FE electron loading was diagnosed first by integral observables like the Q-value, the γ-activity or the electron current picked up by a probe penetrating into the cavity [15]. Specialized diagnostics particular to RF cavities as temperature and X-ray mapping (fig. 7(a,b)) gave at hand more powerful tools for studying individual emitting sites [17], often complementing each other.

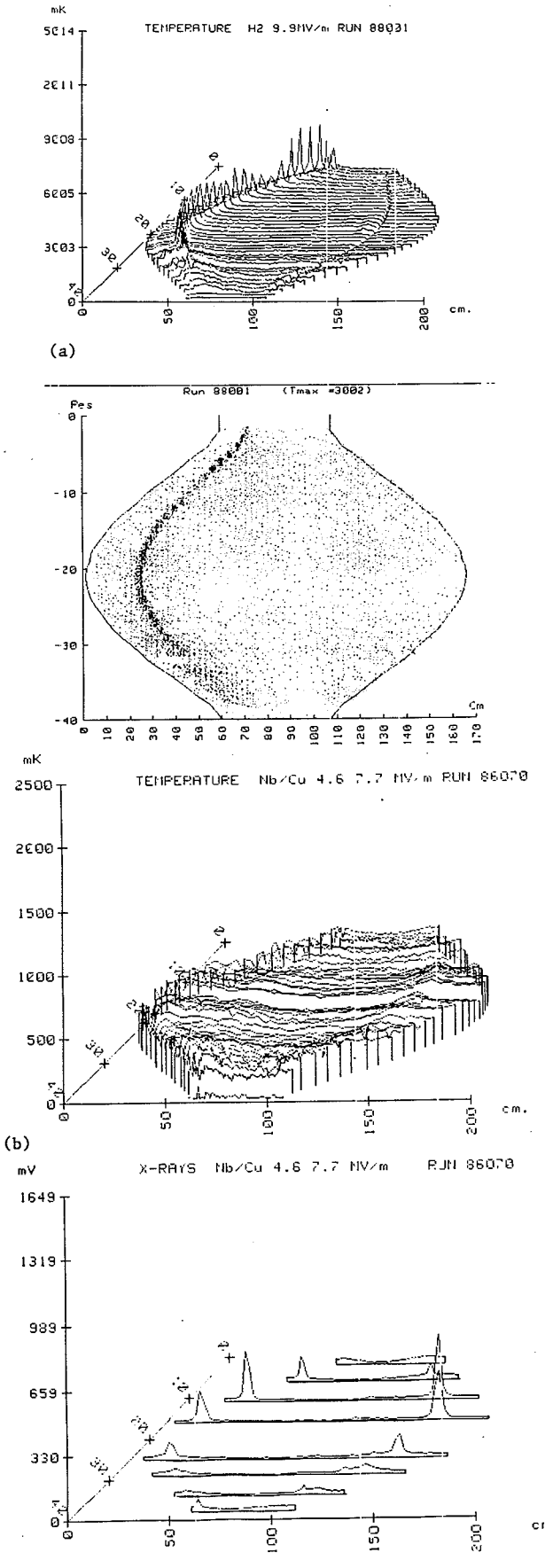

Fig. 7 - (a) Temperature maps of Nb sheet metal cavity at E_a = 10 MV/m and (b) temperature map and X-ray map of a Nb sputter coated Cu-cavity at 7.7 MV/m and 500 MHz.

Fig. 7(b) shows the temperature map of a Nb sputter coated Cu cavity at an accelerating field above the threshold for e^- loading, the temperature signals due to e^- loading being hardly visible. The X-ray mapping, on the contrary, shows a clean signal.

Computer simulations of the electron paths in the electromagnetic field of a cavity allowed to localize the emitter [17]. Emitting sites were found at the cavity bottom (by gravity) and could be traced back to dust particles [18]. Cavity processing techniques were improved thereupon, such that a few time later the emitting sites were no longer concentrated at the bottom of the cavity. It was suggested, that there might be another class of emitters, different from dust, which were intrinsic to the Nb sheet itself [12]. This idea was corroborated later in DC field emission studies on Nb sheet, prepared similarly as the RF cavities. Small micron-size particles, very probably no dust, of different elemental composition were pinned down as emitting sites [19].

Experimental results - A bunch of results originated from the improvement of diagnostical tools [2,3,20,21] and the exchange between groups working in DC FE and those in RF FE.

Features common to both domains are the following:

Pointlike emitters of low spatial density - There are only a few sites on a cm^2. 16 are reported in DC FE for a surface field of 50-60 MV/m, 38 for 90-100 MV/m [19]. Corresponding β-values amount from about 80 to 40 respectively. This observation already suggests a drastic increase of the number of active sites for increasing surface fields (decreasing β-values). 17 emitters were found at an accelerating field of 6 MV/m in a 500 MHz monocell cavity [12]. Taking as the relevant area that one for which the surface electric field is bigger than 90% of the peak surface field (8% of the total surface), this number corresponds to an emitter density of 3.5×10^{-2} on a cm^2 for a β-value of about 330.

Carbon sites as emitters - Carbon in the form of graphite, intentionally deposited onto the surface, emits strongly both in DC [22, 23] and RF [24]. Also artificially introduced MoS_2 particles emit strongly in DC [23].

Fowler-Nordheim current voltage characteristics - The current-voltage (or equivalently the Q-voltage or X-ray intensity-voltage) characteristics follows closely the Fowler-Nordheim law, if the local surface field is by a factor β larger than the average surface field [15,23]. The field enhancement factor β might be considered as a real field enhancement, but also simply as a fit parameter.

From measurements on a coaxial cavity β was found to be constant over seven decades of current, and no frequency dependence of β could be found, the cavity being operated in different modes [25].

Heat treatment - Upon heat treatment at 800°C the number of emitting sites in DC FE is increased, probably by decomposition of organic particles into "carbon sites" or by segregation of material from the bulk [19]. Upon heat treatment above 1200-1400°C the emitter density is drastically reduced , but some emitters are still left [19,26].

Switching - Emitters may appear in two different conductivity states (switching) [26,27]. This observation may explain that in superconducting cavities the accelerating field may initially be increased to higher values, before being reduced by FE electron loading within some minutes [28].

Anodization - The effect on FE electron loading of anodizing the Nb surface is only weak, if present at all [12]. A decrease of the DC FE current with the layer thickness is reported [29]. No significant reduction of the emitter density is noticed [19].

Gas exposure - Exposure to clean laboratory air for short periods does not change the FE activity dramatically [12,19,26]. Exposure to a typical accelerator residual gas mixture gave the following result. At CERN, a cold cavity equipped with an accelerator vacuum beam tube was exposed up to equivalent 5 monolayers of a typical accelerator residual gas atmosphere (H_2:H_2O:CO:CO_2 = 69%:17%:8%:6%). The Q-value (4×10^9 at 4.2 K) did not change. The onset accelerating field of FE electron loading remained constant at 4.9 MV/m to equivalent one monolayer gas exposure, before it decreased to 3.5 MV/m. The pumping capability of the cold cavity surface decreased beyond equivalent one monolayer gas exposure.

Cures against FE emission electron loading

Up till now, He-processing has proved to reduce FE electron loading [30]. An increase of the accelerating field of more than a factor two has been obtained (cf. table 2). Its mechanism is considered to be a selective sputtering of the emitting sites in the RF field of the cavity by He ion impact. Unfortunately, processing times can be very long. At CERN, two LEP prototype cavities had to be processed under He gas for 50 h and 70 h to obtain an accelerating field of 7 MV/m (table 1 and ref. [31]). Sometimes, the progress by He-processing saturates [12].

Recently, very reproducible results on 5-cell 500 MHz cavities to be installed in the TRISTAN collider are reported from KEK [32]. Out of 10 cavities, in 6 the accelerating field E_a could be raised to 10 MV/m within an hour time without He-processing. Fig. 8 shows a typical $Q(E_o)$-curve, no sign of FE electron loading being visible up to 10 MV/m, equivalent to a peak surface field E_p = 20 MV/m. In fig. 9, the inverse Q-value, proportional to the average surface resistance, depends linearly on E_p^2, which is explained by a uniform heating of the cavity surface. The arrows indicate the onset of FE electron loading. The surface treatment these cavities have undergone, differs from what is applied in several other laboratories. The cavities are electropolished, degassed at 700°C (to remove H_2) and rinsed under ultrasonic agitation with pure water under careful control of the conductivity of the supply and outlet water. Only when the conductivity of the drain water has decreased below a threshold value, the rinsing is stopped. There are indications of a correlation of the residual conductivity of the outlet water with the onset of FE electron loading.

Statistical model for FE electron loading - Superconducting cavities of higher frequencies and smaller surface area often show an increased threshold field for electron loading (fig. 3 and fig. 5 in ref. [2]). It is supposed since long, that this fact is due to a smaller probability of having a strong emitter on a small surface [33].

The number of emitters N at an accelerating field E_a and a frequency f is to be calculated for a multicell cavity composed from n single cells. Free parameters are the surface density s of the (active or passive) emitters and the probability density of β-values p(β). The condition $\int_{\beta min}^{\beta max} d\beta\ p(\beta) = 1$ holds, β_{min} and β_{max} being the minimum and maximum β-value. Whether an emitting site is active or not is decided from its β-value and the average local surface field E_i, to which it is exposed. It is active if $\beta E_i > E_{th}$. E_{th} is the threshold field for electron loading, determined from a series of 500 MHz monocell cavity measurements, for which the current picked up by a probe exceeds 10 pA (fig. 10): E_{th} = 4 GV/m. The total cavity surface is subdivided into k surface area elements A_i, at which the average local surface field E_i is supposed to be constant. In that case an emitter with a field enhancement factor β is exposed to the surface field βE_i. Hence, the number of active emitters N_i on the surface element i is

$$N_i = \int_{\beta_{min}}^{\beta_{max}} d\beta\ p(\beta)\ s\ A_i\ \Theta(\beta E_i - E_{th})$$

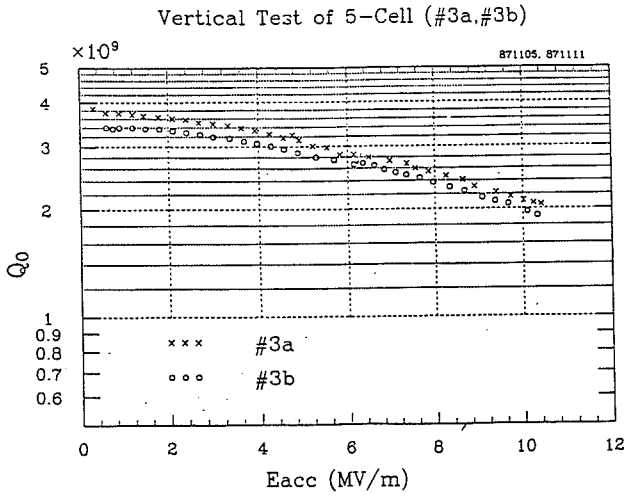

Fig. 8 - Dependence of the Q-value on the accelerating field for a 5-cell 500 MHz cavity from KEK.

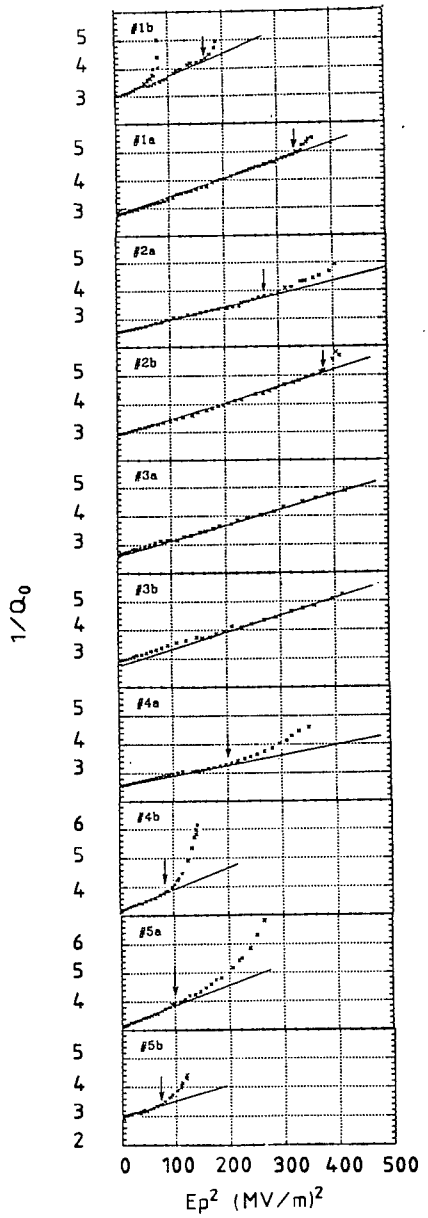

Fig. 9 - Dependence of cavity losses on the peak surface field E_p. The quadratic dependence proves uniform heating of the surface. The onset of electron loading is marked by an arrow.

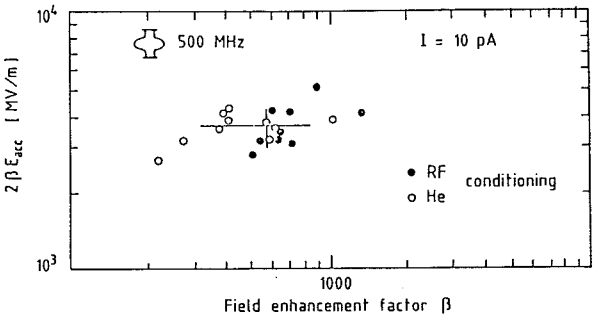

Fig. 10 - Threshold field $E_{th} = 2\beta E_{acc}$ for which the electron current picked up by a current probe at the cavity beam tube exceeds 10 pA.

$\Theta(x) = 0$ for $x < 0$ and 1 for $x \geq 0$. A_i scales with the frequency as $A_i \sim f^{-2}$. The total number of emitters is a function of E_a and f,

$$N(E_{a,f}) = \sum_{i=1}^{k} \int_{\beta_{min}}^{\beta_{max}} d\beta\, p(\beta)\, s\, A_i(f)\, \Theta[\beta E_i(E_a) - E_{th}]$$

The threshold accelerating field for the start-up of FE electron loading E_a^{max} is determined from the condition $N(E_a^{max}) = 1$. $p(\beta)$ is chosen close to the experimentally determined emitter density for $\beta = 40$, 80 and 330 (see before).

The parameters $\beta_{min} = 50$, $\beta_{max} = 1000$, $s = 1000\ m^{-2}$, and $p(\beta) \sim 10^{-\beta/100}$ give the result of table 3.

TABLE 3 - Statistical model for FE electron loading

f [MHz]	n	E_a^{max} [MV/m] (a)	(b)	Ref.
3000	1	27	25	[34]
500	1	11	15.1	(c)
500	5	7.8	10.0	[32]
350	1	8.8	10.9	[13]
350	4	7.3	7.5	[35]

(a) Calculated.
(b) Experimentally obtained.
(c) This paper.

Hence, a statistical model is not ruled out. It is interesting to note that within this simple model it is not possible to represent the experimental data with a $p(\beta)$ distribution much different from the exponential one used. This might be another indication of a strong increase of $p(\beta)$ towards lower β values or equivalently a strong increase of the number of emitting sites with the accelerating field, already stated before as an

experimental result. Furthermore, that might be the cause of the occasional observation, that the progress by the processing tends to saturate.

CONCLUSION

The main obstacle towards accelerating fields higher than 10 MV/m is electron loading. MP electron loading may limit the accelerating fields, but can be processed away. However, processing times might be long. There exists experimental evidence, that accelerating fields of 10 MV/m can reproducibly be obtained in storage ring accelerating multicell structures. New diagnostical tools developed for superconducting RF cavities have contributed to the knowledge of electron emission on broad areas. Experimental results in DC and RF field emission are very similar. A simple statistical model, with an exponential increase of the number of emitters towards lower β-values, may explain the frequency dependence of FE electron loading observed so far.

ACKNOWLEDGEMENTS

I would like to thank my colleagues from CERN and also Prof. Y. Kojima and his collaborators on the occasion of my visit to KEK for many fruitful discussions and information.

REFERENCES

[1] T. Yogi et al., Phys. Rev. Lett. 39 (1977) 826.

[2] G. Müller, Proc. of the 3rd Workshop on RF Superconductivity, Argonne, September 1987, Ed. K.W. Shepard, p. 331.

[3] H. Piel, Proc. of the 1st Workshop on RF Superconductivity, Karlsruhe, July 1980, Ed. M. Kuntze, p. 85.

[4] G. Müller, Proc. of the 2nd Workshop on RF Superconductivity, Geneva, July 1984, Ed. H. Lengeler, p. 377.

[5] H. Padamsee, IEEE Trans. Magn. MAG-23 (1987) 1607.

[6] C. Benvenuti et al., ibid. ref. 2, p. 445.

[7] Ph. Bernard et al., European Particle Accelerator Conf., Rome (1988) (in preparation).

[8] C.M. Lyneis et al., Appl. Phys. Lett. 31 (1977) 541.

REFERENCES (Cont'd)

[9] V. Lagomarsino et al., IEEE Trans. Mag. MAG-15 (1979) 25.

[10] U. Klein and D. Proch, Proc. Conf. Future Possibilities of Electron Accelerators, Charlottesville, USA (1979).

[11] R. Calder et al., Nucl. Instr. Meth. B13 (1986) 631.

[12] W. Weingarten, ibid. ref. 4, p. 551.

[13] D. Bloess et al., CERN/EF/RF 85-2.

[14] M. Lavarec et al., Proc. 8th Int. Symp. on Discharges and Electr. Insul. Vac., Albuquerque (1978) p. C3-1.

[15] S. Noguchi et al., Nucl. Instr. Meth. 179 (1981) 205.

[16] R.J. Noer, Appl. Phys. A28 (1982) 1.

[17] Ph. Bernard et al., Nucl. Instr. & Meth. 190 (1981) 257.

[18] Ph. Bernard et al., Nucl. Instr. & Meth. 206 (1983) 47.

[19] Ph. Niedermann et al., J. Appl. Phys. 59 (1986) 892.

[20] C.E. Reece, ibid. ref. [2], p. 545.

[21] P. Kneisel et al., IEEE Trans. Magn. MAG-23 (1987) 1417.

[22] C.S. Athwal et al., IEEE Trans. Plasma Sci 13 (1985) 226.

[23] R.J. Noer et al., J. Appl. Phys. 59 (1986) 3851.

[24] C. Athwal and W. Weingarten, CERN/EF/RF 84-7.

[25] U. Klein and J. Turneaure, IEEE Trans. Magn. MAG-19 (1983) 1330.

[26] H. Padamsee et al., ibid. ref. [2], p. 251.

[27] R.V. Latham, ibid. ref. [4], p. 533.

[28] Ph. Bernard et al., CERN/EF/RF 81-2.

[29] G. Sayag et al., J. Phys. E10 (1977) 176.

[30] H.A. Schwettman et al., J. Appl. Phys. 45 (1974) 914.

[31] G. Arnolds-Mayer et al., IEEE Trans. Nucl. Sci. NS-32 (1985) 3587.

[32] Y. Kojima, private communication.

[33] C. Lyneis et al., IEEE Trans. Nucl. Sci. NS-20 (1973) 101.

[34] G. Müller et al., this conference.

[35] G. Arnolds-Mayer et al., ibid. ref. 2, p. 55.